Available online at www.sciencedirect.com
SCIENCE DIRECT
Biochimica et Biophysica Acta 1744 (2005) 19–28
BIOCHIMICA ET BIOPHYSICA ACTA
BBA
http://www.elsevier.com/locate/bba

Mitochondria are intracellular magnesium stores: investigation by simultaneous fluorescent imagings in PC12 cells

Takeshi Kubota[a], Yutaka Shindo[a], Kentaro Tokuno[a], Hirokazu Komatsu[b], Hiroto Ogawa[c], Susumu Kudo[d], Yoshiichiro Kitamura[a], Koji Suzuki[b,e], Kotaro Oka[a,*]

[a]*School of Fundamental Science and Technology, Keio University, 3-14-1 Hiyoshi, Kohoku-ku, Yokohama, Kanagawa 223-8522, Japan*
[b]*Department of Applied Chemistry, Keio University, Kanagawa, Japan*
[c]*Department of Biology, Saitama Medical School, Saitama, Japan*
[d]*Department of Mechanical Engineering, Shibaura Institute of Technology, Tokyo, Japan*
[e]*JST-CREST, Saitama, Japan*

Received 12 August 2004; received in revised form 14 October 2004; accepted 15 October 2004
Available online 11 November 2004

Abstract

To determine the nature of intracellular Mg^{2+} stores and Mg^{2+} release mechanisms in differentiated PC12 cells, Mg^{2+} and Ca^{2+} mobilizations were measured simultaneously in living cells with KMG-104, a fluorescent Mg^{2+} indicator, and fura-2, respectively. Treatment with the mitochondrial uncoupler, carbonyl cyanide *p*-(trifluoromethoxy) phenylhydrazone (FCCP), increased both the intracellular Mg^{2+} concentration ($[Mg^{2+}]_i$) and the $[Ca^{2+}]_i$ in these cells. Possible candidates as intracellular Mg^{2+} stores under these conditions include intracellular divalent cation binding sites, endoplasmic reticulum (ER), Mg-ATP and mitochondria. Given that no change in $[Mg^{2+}]_i$ was induced by caffeine application, intracellular IP_3 or Ca^{2+} liberated by photolysis, it appears that no Mg^{2+} release mechanism thus exists that is mediated via the action of Ca^{2+} on membrane-bound receptors in the ER or via the offloading of Mg^{2+} from binding sites as a result of the increased $[Ca^{2+}]_i$. FCCP treatment for 2 min did not alter the intracellular ATP content, indicating that Mg^{2+} was not released from Mg-ATP, at least in the first 2 min following exposure to FCCP. FCCP-induced $[Mg^{2+}]_i$ increase was observed at mitochondria localized area, and vice versa. These results suggest that the mitochondria serve as the intracellular Mg^{2+} store in PC12 cell. Simultaneous measurements of $[Ca^{2+}]_i$ and mitochondrial membrane potential, and also of $[Ca^{2+}]_i$ and $[Mg^{2+}]_i$, revealed that the initial rise in $[Mg^{2+}]_i$ followed that of mitochondrial depolarization for several seconds. These findings show that the source of Mg^{2+} in the FCCP-induced $[Mg^{2+}]_i$ increase in PC12 cells is mitochondria, and that mitochondrial depolarization triggers the Mg^{2+} release.

Keywords: Magnesium; Mitochondria; KMG; Photolysis; FCCP; Fluorescent imaging

1. Introduction

The magnesium ion, Mg^{2+}, is an important divalent cation in cells, serving to stabilize nucleic acid and protein structure [1,2], blocking a number of different ion channel types [3–6] and mediating Mg^{2+}-dependent enzymatic reactions as a cofactor [7–9], including ATP-related enzymatic reactions [10,11]. Given these important functions, it is evident that perturbations in the intracellular Mg^{2+} concentration, $[Mg^{2+}]_i$, could have serious implications for the proper physiological functioning of cells. Some age-related and neuronal diseases are known to be related to

Abbreviations: caged Ca^{2+}, nitrophenyl EGTA; JC-1, 5,5′,6,6′-tetrachloro-1,1′,3,3′-tetraethylbenzimidazolylcarbocyanine iodide; FCCP, carbonyl cyanide *p*-(trifluoromethoxy) phenylhydrazone; KMG-104, 1-(2,7-difluoro-6-hydroxy-3-oxo-3*H*-xanthen-9-yl)-4-oxo-4*H*-quinolizine-3-carboxylic acid; EPMA, electron probe microanalysis; IP_3, inositol 1,4,5-trisphosphate; Ψ_{Mt}, mitochondrial membrane potential; PD, Parkinson's disease

* Corresponding author. Tel.: +81 45 563 1151x43330; fax: +81 45 564 5095.
E-mail address: oka@bio.keio.ac.jp (K. Oka).

0167-4889/$ - see front matter © 2004 Elsevier B.V. All rights reserved.
doi:10.1016/j.bbamcr.2004.10.013

a deficiency of Mg^{2+} [12–14]. For example, the $[Mg^{2+}]_i$ of rat smooth muscle and human red blood cells from hypertensives is lower than that of normotensive controls [15,16]. Patients with diabetes mellitus also have low serum $[Mg^{2+}]$ [17]. On this basis, it is important to know more about intracellular Mg^{2+} mobilizations in order to shed light on possible mechanisms or causes of these diseases.

$[Mg^{2+}]_i$ is usually maintained around 1 mM at rest in mammalian cells [7]. One of known Mg^{2+} mobilization mechanisms for the maintenance of $[Mg^{2+}]_i$ is Mg^{2+} exchange at the cell membrane. A Na^+/Mg^{2+} exchanger located on the cell membrane has been described for various cell types and it has been reported that $[Mg^{2+}]_i$ depends on the extracellular Na^+ concentration [18–21]. Mg^{2+} efflux is observed in response to an increase in the extracellular concentration of Na^+ or Ca^{2+} in rat liver plasma membranes [22,23]. The Na^+/Mg^{2+} exchanger is known to be inhibited by amiloride or imipramine [21,23], and it has been reported that the recovery of $[Mg^{2+}]_i$ to normal levels in PC12 cells was suppressed by imipramine after a transient increase induced by the mitochondrial uncoupler, carbonyl cyanide *p*-(trifluoromethoxy) phenylhydrazone (FCCP) [24]. While the main focus of these reports has been on Mg^{2+} translocation through the cell membrane, the issue of intracellular Mg^{2+} releasing points has received less attention.

The FCCP-induced increase in $[Mg^{2+}]_i$ has been described for a variety of cell types [24–26] and is also observed in cells bathed in Mg^{2+}-free media [26]. Given that $[Mg^{2+}]_i$ accounts for less than 5% of the total cellular Mg^{2+} (~20 mM) [7], these findings suggest that almost all intracellular Mg^{2+} exists in bound form or is sequestered within organelles, and that cells therefore possess endogenous Mg^{2+} releasing mechanisms [26]. The purpose of this study is to determine the source of Mg^{2+} in the FCCP-induced increase in $[Mg^{2+}]_i$ of PC12 cells.

FCCP also induces an increase in $[Ca^{2+}]_i$ [27,28]. Ca^{2+} is usually accumulated in the endoplasmic reticulum (ER) of cells, and released through ryanodine receptors and/or via ligand-gated inositol 1, 4, 5-trisphosphate (IP_3) receptors [29–31]. Ca^{2+}-induced Ca^{2+} release (CICR) mechanisms are also responsible for the release of Ca^{2+} from intracellular organelles. If a similar release mechanism exists for Mg^{2+}, then Ca^{2+} inducible stimuli might induce Mg^{2+} release through ion channel receptors. Another possibility concerns that of Mg^{2+} substitution. Many divalent cation binding sites are present in the cell, such as DNA and RNA [1,2]. EF-hand of troponin C has affinity for both Mg^{2+} and Ca^{2+}, and the binding is competitive [32,33]. Furthermore, it has been reported that most of the proteins which interact with Ca^{2+} can also interact with Mg^{2+} [34]. A strong Ca^{2+} increase may preferentially interact with binding sites and liberate Mg^{2+} from those binding sites in the cell.

ATP synthesis in cells is inhibited by FCCP treatment. When ATP, which binds strongly to Mg^{2+} and mainly exists as an Mg-ATP complex in cells, decomposes to ADP with energy release, free Mg^{2+} will be released to the cytosol. Therefore, ATP depletion by FCCP could induce an increase in $[Mg^{2+}]_i$.

It has been revealed by electron probe micro analysis (EPMA) that mitochondria contain Mg^{2+} [35,36]. Mitochondria are also known as Ca^{2+} stores [37–39], and FCCP induces an increase in $[Ca^{2+}]_i$ via Ca^{2+} release from these organelles. Therefore, Mg^{2+} release from mitochondria is plausible upon FCCP-induced mitochondrial membrane depolarization.

Possible candidates for Mg^{2+} release points include the ER, intracellular divalent binding sites, Mg-ATP, and mitochondria. In this regard, we have examined here Mg^{2+} storage and release properties of PC12 cells, and have made simultaneous Mg^{2+}-Ca^{2+} measurements to investigate Mg^{2+} mobilization mechanisms in these cells.

2. Materials and methods

2.1. Chemical reagents and cell culture

Dulbecco's modified Eagle's medium (DMEM), horse serum (HS), and fetal bovine serum (FBS) were purchased from GIBCO (MD, USA). The free acid form of fura-2, its acetoxymethyl ester form (fura-2-AM), nitrophenyl EGTA-AM (caged Ca^{2+}-AM), 5,5′,6,6′-tetrachloro-1,1′,3,3′-tetraethylbenzimidazolylcarbocyanine iodide (JC-1), caged IP_3 and MitoFluor™ Red 589 were from Molecular Probes (OR, USA). Oligomycin was from Calbiochem (CA, USA). Poly-D-lysine (PDL), nerve growth factor (NGF), carbonyl cyanide *p*-(trifluoromethoxy) phenylhydrazone (FCCP), and other reagents were from Sigma (MO, USA). The free acid and AM forms of 1-(2,7-difluoro-6-hydroxy-3-oxo-3*H*-xanthen-9-yl)-4-oxo-4*H*-quinolizine-3-carboxylic acid (KMG-104) were developed and synthesized as highly selective fluorescent Mg^{2+} indicators [40,41]. PC12 cells [42] were obtained from RIKEN Tsukuba Institute; cells were cultured at 37°C in DMEM containing heat-inactivated serums (10% HS, 5% FBS), 25 U/ml penicillin and 25 μg/ml streptomycin, under a humidified atmosphere with 5% CO_2. For experimental use, cells (passage number 5–9) were cultured on glass coverslips coated with PDL, and differentiated by culturing with 50 ng/ml NGF-containing serum-free medium for 5–7 days.

2.2. KMG-104 is a novel Mg-specific fluorescent indicator

KMG-104, which has a fluorescein chromophore, is an up-to-date version of the KMG series of Mg^{2+} probes [40,41,43]. The fluorescence intensity of KMG-104 increases largely with increasing $[Mg^{2+}]$ and shows no response to Na^+ and K^+, the main intracellular cations. The K_d for Mg^{2+} is about 2.1 mM, which is near to the physiological concentration of Mg^{2+} [40,41]. The most outstanding point of this indicator is its selectivity for Mg^{2+}

over Ca^{2+}. Because other conventional Mg^{2+} indicators have moderate affinities for Ca^{2+} (K_dCa (μM) of Magnesium Green, 7; Mag-fura-5, 31; Mag-indo-1, 29) [44], they can also be used as Ca^{2+} indicators at high $[Ca^{2+}]$. The K_d of KMG-104 for Ca^{2+} is about 7.5 mM which is much higher than the resting physiological $[Ca^{2+}]_i$. The fluorescence of KMG-104 also has a low sensitivity to pH change in the range from 6.0 to 7.6 [40,41]. This newly developed Mg^{2+} indicator has the potential to become a potent tool for investigating physiological roles of Mg^{2+}. For the double staining method described here, it was important to choose suitable indicators that were highly selective for respective

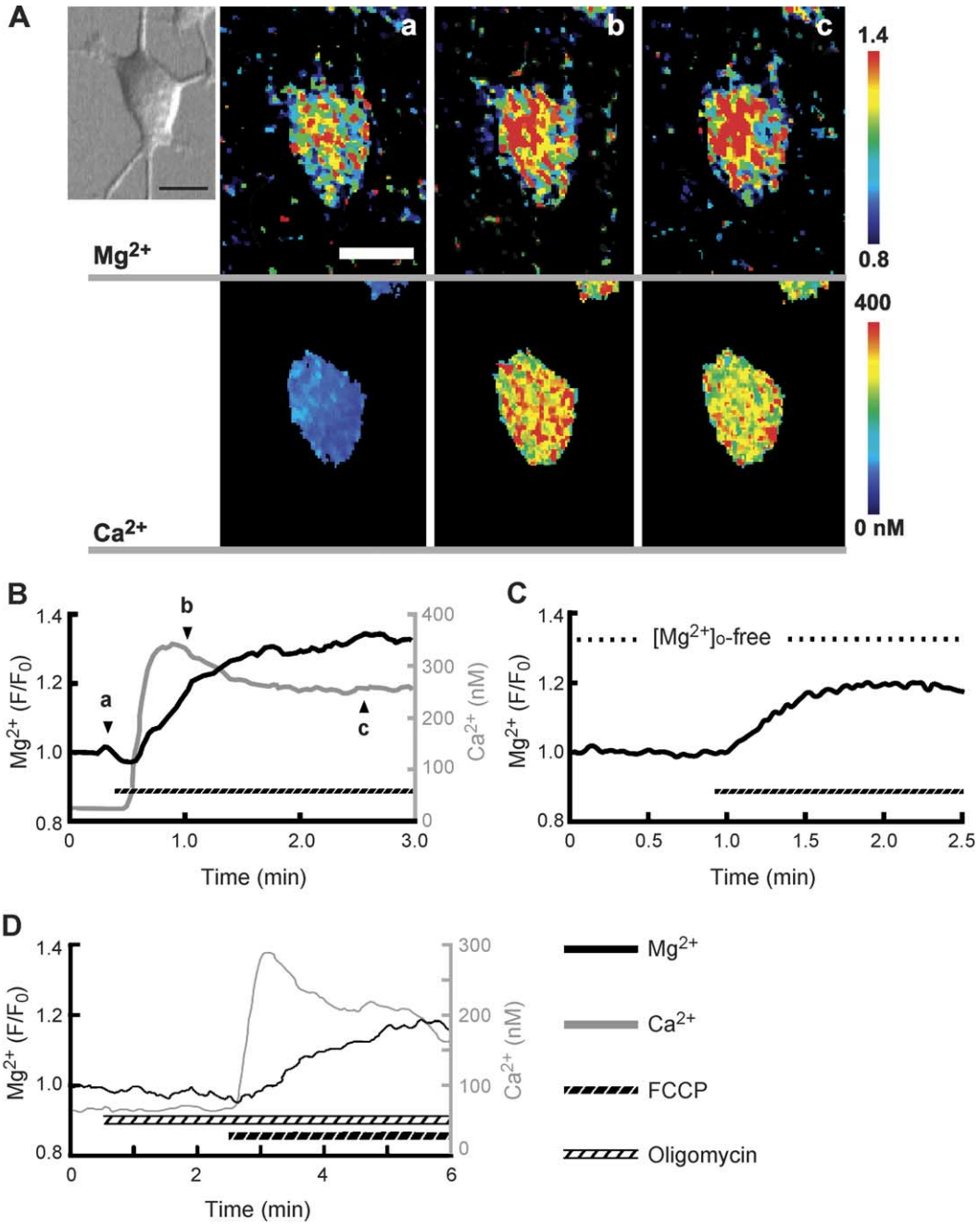

Fig. 1. FCCP induces an increase in $[Mg^{2+}]_i$. KMG-104-AM and fura-2-AM-loaded PC12 cells were treated with FCCP. (A) DIC image and pseudo colored images of differentiated PC12 cells. Simultaneous images are for KMG-104 (upper) and for fura-2 (bottom). Both $[Mg^{2+}]_i$ and $[Ca^{2+}]_i$ increased in response to FCCP treatment. The scale bars in the images indicate 10 μm. (B) Time courses of $[Mg^{2+}]_i$ and $[Ca^{2+}]_i$ responses. Bath application of 5 μM FCCP (striped line) induced an increase in both $[Mg^{2+}]_i$ (black line) and $[Ca^{2+}]_i$ (grey line). Arrowheads (a–c) correspond with those of A. (C) $[Mg^{2+}]_i$ response in Mg^{2+}-free buffer. Application of 5 μM FCCP (striped line) induced $[Mg^{2+}]_i$ increase even in the absence of extracellular Mg^{2+}. (D) Time courses of changes in $[Mg^{2+}]_i$ and $[Ca^{2+}]_i$ in response to FCCP treatment after 2-min incubation with oligomycin. Oligomycin inhibits the breakdown of ATP on the mitochondrial inner membrane. Application of 5 μM FCCP (black-based striped line) in the presence of 10 μM oligomycin (white-based striped line) also induced increases in both $[Mg^{2+}]_i$ and $[Ca^{2+}]_i$.

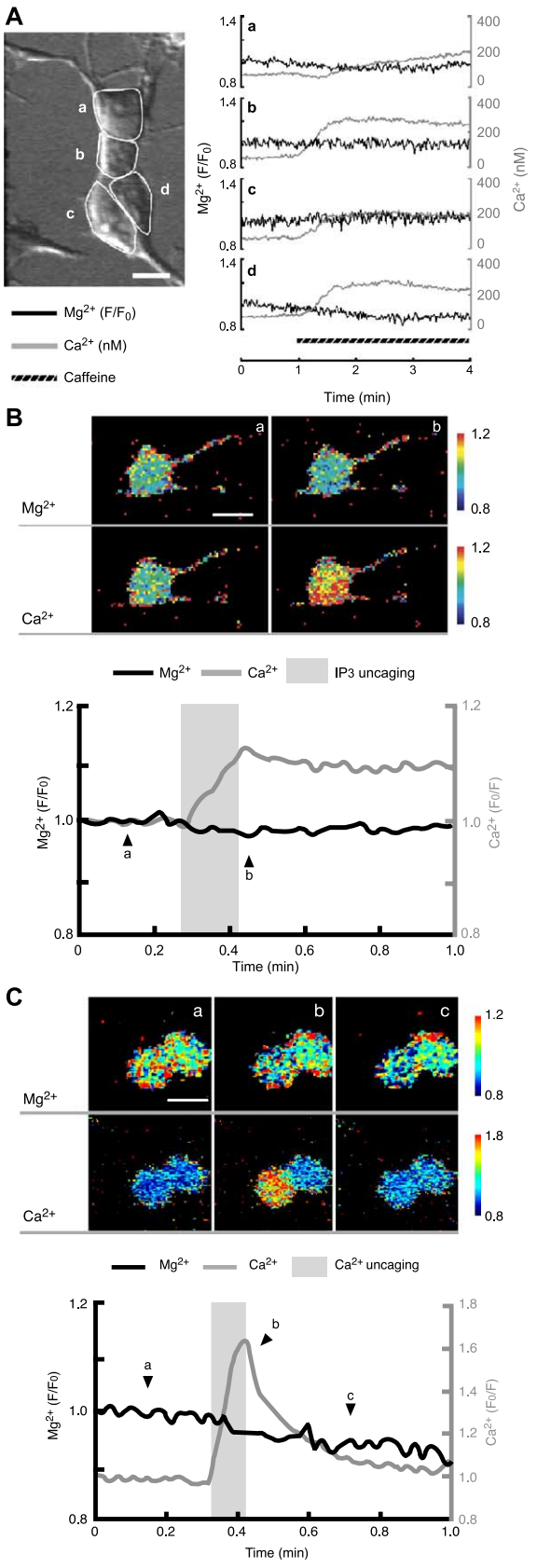

ions and could be clearly distinguishable in terms of their optical characteristics. KMG-104 and fura-2 were an appropriate combination that satisfied such a requirement.

2.3. Dye loading

KMG-104-AM was stored at <0 °C as a 10 mM stock solution in DMSO. For optical imaging, cells were incubated with 10 μM KMG-104-AM in the culture medium for 30 min at 37 °C, and then washed twice with a recording (normal) solution containing (in mM): NaCl, 125; KCl, 5; $MgSO_4$, 1.2; $CaCl_2$, 2; KH_2PO_4, 1.2; glucose, 6; HEPES, 25 (pH 7.4); and further incubated for 15 min to allow for complete hydrolysis of the acetoxymethyl ester form in the cells. A coverslip with dye-loaded cells was then set in an experimental chamber (RC-25F, Warner Instrument Corp.). Loading of other cell permeable reagents, 2 μM fura-2-AM, 10 μM NP-EGTA-AM as mixtures with 0.02% pluronic F-127, was carried out at the same time. Localization of mitochondrion was visualized with MitoFluor™ Red 589. KMG-104 loaded cells were further incubated with 500 nM MitoFluor™ Red 589 for 15 min. Mitochondrial membrane potential was monitored with a spectrum shift type fluorescent dye, JC-1. Cells were incubated for 15 min in normal solution containing 10 mg/ml JC-1, and washed twice. Cell membrane-impermeable reagents were microinjected into PC12 cells with a glass micropipette (tip diameter <1 μm). The concentrations of caged IP_3, KMG-104-free acid and fura-2-free acid in the pipette were 0.5, 5, and 1 mM, respectively. Loading of the reagents was confirmed by the presence of their respective fluorescences. The Ca^{2+} response at this time was measured with 380-nm excitation light only.

Fig. 2. Neither ER-derived Ca^{2+} nor direct $[Ca^{2+}]_i$ elevation caused an increase in $[Mg^{2+}]_i$. (A) $[Mg^{2+}]_i$ and $[Ca^{2+}]_i$ changes induced by caffeine, a ryanodine receptor agonist. DIC image of four cells is displayed at left. Application of 10 mM caffeine (black-based striped line at bottom of figure) induced an increase in $[Ca^{2+}]_i$ in all cells (a–d), each with a slightly different response pattern (grey lines). $[Mg^{2+}]_i$ did not increase in any of the cells (black lines). White circles in DIC image indicate ROIs. The scale bar indicates 10 μm. (B) $[Mg^{2+}]_i$ and $[Ca^{2+}]_i$ responses induced by IP_3. Caged IP_3 and the two fluorescence indicators were microinjected into the cell. Sequential images of $[Mg^{2+}]_i$ (left top) and $[Ca^{2+}]_i$ (left bottom) responses and time courses of change (right). The scale bar signifies 10 μm. Laser flashes on the center of the cell body induced an increase in $[Ca^{2+}]_i$ (grey line), while $[Mg^{2+}]_i$ did not change (black line). Grey area indicates a set of five photolysis flashes. The timings of arrowheads (a and b) correspond to the fluorescence images. Ca^{2+} responses were displayed as F_0/F in B and C since fura-2 was excited at 380-nm wavelength in the experiments. (C) $[Mg^{2+}]_i$ and $[Ca^{2+}]_i$ responses induced by direct $[Ca^{2+}]_i$ elevation. Cells were loaded with caged Ca^{2+} (NP-EGTA) and the two indicators. Sequential images of $[Mg^{2+}]_i$ (left top) and $[Ca^{2+}]_i$ (left bottom) responses and time courses of change (right). The scale bar signifies 10 μm. Laser flashes on the center of the left cell body induced an increase in $[Ca^{2+}]_i$ (grey line), while $[Mg^{2+}]_i$ did not change (black line). Grey area indicates a set of five photolysis flashes. The timings of arrowheads (a–c) correspond to the fluorescence images.

2.4. Fluorescent measurements

The excitation light wavelength used for KMG-104 was 480 nm, while for fura-2 wavelengths of 340 and/or 380 nm were used. Fluorescence images were acquired with an inverted microscope (ECLIPSE TE300, Nikon) equipped with an objective (×20, ×40; S Fluor, or ×60; Plan Apo, Nikon), a 505 dichroic mirror and a 535/55-nm barrier (green) filter. Mg^{2+} responses were presented as $F/F_0=(f-b)/(f_0-b_0)$, where f and b are fluorescent intensity from the cell and background, respectively, at any given time point, and f_0 and b_0 are fluorescent intensity from the cell and background at the beginning of the experiment. Fluorescence ratios (340/380) were converted to $[Ca^{2+}]_i$ following a conventional calibration method [45]. MitoFluor™ Red 589 accumulates in mitochondria regardless of the mitochondria's membrane potential. MitoFluor™ Red 589 was excited at 560 nm and fluorescence obtained with 575-nm dichroic mirror and 600-nm long pass filter. JC-1 is a dual-emission probe that shows a fluorescence emission shift from green to red, with the ratio of green to red fluorescence corresponding to membrane potential. JC-1 shows red fluorescence by J-aggregation in mitochondria [46]. An increase in the fluorescence ratio (green/red fluorescence) indicates depolarization of the mitochondrial membrane potential. JC-1 was excited at 490 nm and fluorescence measured simultaneously with a double view system (Hamamatsu Photonics) equipped with a 590-nm dichroic mirror, the green filter and a 600LP (red) filter. A Xe lamp (150 W) with a monochromator unit was used for multiple excitations, and fluorescence measured sequentially with a CCD camera (HiSCA, Hamamatsu Photonics). The fluorescence was calculated as the mean intensity over a defined region of interest (ROI).

In vivo calibration of resting $[Mg^{2+}]_i$ was performed following Sharikabad's method [47]. To equilibrate extra- and intracellular $[Mg^{2+}]$, cells were incubated in 0 and 100 mM Mg^{2+} containing KRH solution with 50 μM calcimycin for 3 h. Then, cells were stained with KMG-104-AM, and fluorescent intensities were obtained as minimum (F_{min}) and maximum (F_{max}) intensities, respectively. $[Mg^{2+}]_i$ at rest was calculated following a conventional formula for single excitation dyes: $[Mg^{2+}]=K_d(F-F_{min})/(F_{max}-F)$, here, 2.1 mM was used for K_d [40,41]. Calculated $[Mg^{2+}]_i$ in resting PC12 cell was 0.9±0.1 mM (value from each 90 cells).

2.5. Laser photolysis

Caged compounds were photoreleased by several flashes elicited by a YAG pulse laser (355 nm, 7 mJ). The diameter of the laser spot was 3–5 μm in the focal plane with a ×20 objective. On account of the different setups required, the laser photolysis technique and 340-nm excitation for fura-2 could not be used at the same time.

2.6. Estimation of intracellular [ATP]

The intracellular ATP concentration ($[ATP]_i$) was estimated by luciferin–luciferase assay [48] following a slightly modified method of Kudo et al. [49]. Briefly, after treatment with FCCP (0, 2, 30 min), cells were washed twice with ice-cold PBS. Cells were then scraped from dishes into vials and centrifuged at 2600×g for 4 min. Ice-cold distilled water was then replaced with the PBS, and cells were frozen in a deep freezer (−80 °C). At the time of experiments, the vials were placed floating in boiling water for 10 min and then centrifuged at 2600×g for 5 min. The supernatant was used for estimation of [ATP] and protein content. [ATP] was estimated using an ATP determination kit (Molecular Probes) with a micro-plate-reader (Ascent Fluoroskan, DAINIPPON). Protein concentration was estimated following the method of Bradford using Coomassie brilliant blue [50]. $[ATP]_i$ was normalized to nmol/mg protein. Data were analyzed by Student's t tests. N and n in this paper mean number of dishes and number of cells in the dishes, respectively.

3. Results

3.1. What is the origin of Mg^{2+} following FCCP treatment?

We have previously reported that FCCP induces an increase in $[Mg^{2+}]_i$ in PC12 cells [24]. Here, PC12 cells double-stained with KMG-104-AM and fura-2-AM were treated with 5 μM FCCP which induced an increase in both $[Ca^{2+}]_i$ and $[Mg^{2+}]_i$ (N=9, Fig. 1A and B). Because $[Ca^{2+}]_i$ and $[Mg^{2+}]_i$ also increased by treatment with FCCP in the Mg-free buffer (Fig. 1C), PC12 cells have intracellular Mg^{2+} stores and Mg^{2+} releasing mechanism.

3.2. ER stimulation does not induce Mg^{2+} release

Double-stained PC12 cells were stimulated with caffeine (10 mM), an agonist of ER membrane-bound ryanodine receptors. This induced an increase in $[Ca^{2+}]_i$ (Fig. 2A) which was long-lasting in the presence of the caffeine (grey lines). $[Mg^{2+}]_i$ did not increase during these Ca^{2+} responses (black lines, N=5). IP_3 receptors were subsequently activated by IP_3 liberated by the photolysis of caged IP_3. This was achieved by a series of five laser flashes, for which the liberated IP_3 induced successive increases in $[Ca^{2+}]_i$ only (N=4, Fig. 2B). $[Mg^{2+}]_i$, and thus release of Mg^{2+} from the ER did not change in response to these two procedures to induce ER Ca^{2+} release.

3.3. Ca^{2+} does not induce Mg^{2+} release from divalent cation binding sites

Caged Ca^{2+} was used to investigate the effect of direct $[Ca^{2+}]_i$ elevation on $[Mg^{2+}]_i$. PC12 cells were incubated

with the AM forms of KMG-104, fura-2, and caged Ca^{2+}. Ca^{2+} liberation by several exposures to UV laser flashes resulted in an increase in $[Ca^{2+}]$ (Fig. 2C). The Ca^{2+} responses were also observed several times in succession in the one cell. During these trials, $[Mg^{2+}]_i$ did not change (N=6). These results show that, under both physiological or nonphysiological $[Ca^{2+}]_i$ conditions, Ca^{2+} did not displace Mg^{2+} from any binding sites, and showed the lack of sensitivity of KMG-104 fluorescence to changes in $[Ca^{2+}]_i$.

3.4. Mg^{2+} is not released from Mg-ATP complexes

On the basis of the above findings, Mg-ATP and the mitochondria remain as the most likely candidates as Mg^{2+} stores in PC12 cells. The mitochondrial membrane potential (Ψ_{Mt}) is depolarized by the effect of FCCP, in which case mitochondrial ATP synthase acts in reverse to decompose ATP. Mg^{2+} should be released from Mg-ATP on account of this vigorous ATP consumption. We used oligomycin, an inhibitor of Fo ATP synthase, to eliminate the possibility of release of Mg^{2+} from Mg-ATP upon depolarization of the mitochondrial membrane potential. When FCCP was applied 2 min after incubation with oligomycin (10 μM), $[Mg^{2+}]_i$ did not initially increase, but $[Mg^{2+}]_i$ and $[Ca^{2+}]_i$ gradually increased with continued exposure to FCCP (N=3, Fig. 1D). Furthermore, $[ATP]_i$, which was measured before and then 2 min after FCCP treatment (Fig. 3), did not undergo any significant change. It did decrease significantly after 30-min incubation with FCCP. From these results, it was confirmed that Mg^{2+} was not released from Mg-ATP complexes, at the least in the initial 2 min after FCCP exposure.

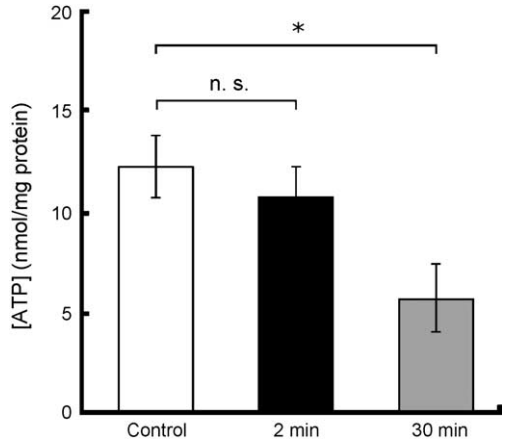

Fig. 3. Estimation of intracellular ATP concentrations before and after FCCP treatment. ATP concentrations of PC12 cells for each condition were measured by luciferin–luciferase assay. Control is the [ATP] before FCCP treatment (white bar). This was compared with [ATP] in FCCP-exposed cells (2 min FCCP, black bar) and [ATP] in cells following a long exposure to FCCP (30 min FCCP, grey bar). [ATP] is reported as nmol/mg protein. Error bars show S.E., and asterisk signifies P<0.01 versus Control (N=20, 22, 15, respectively).

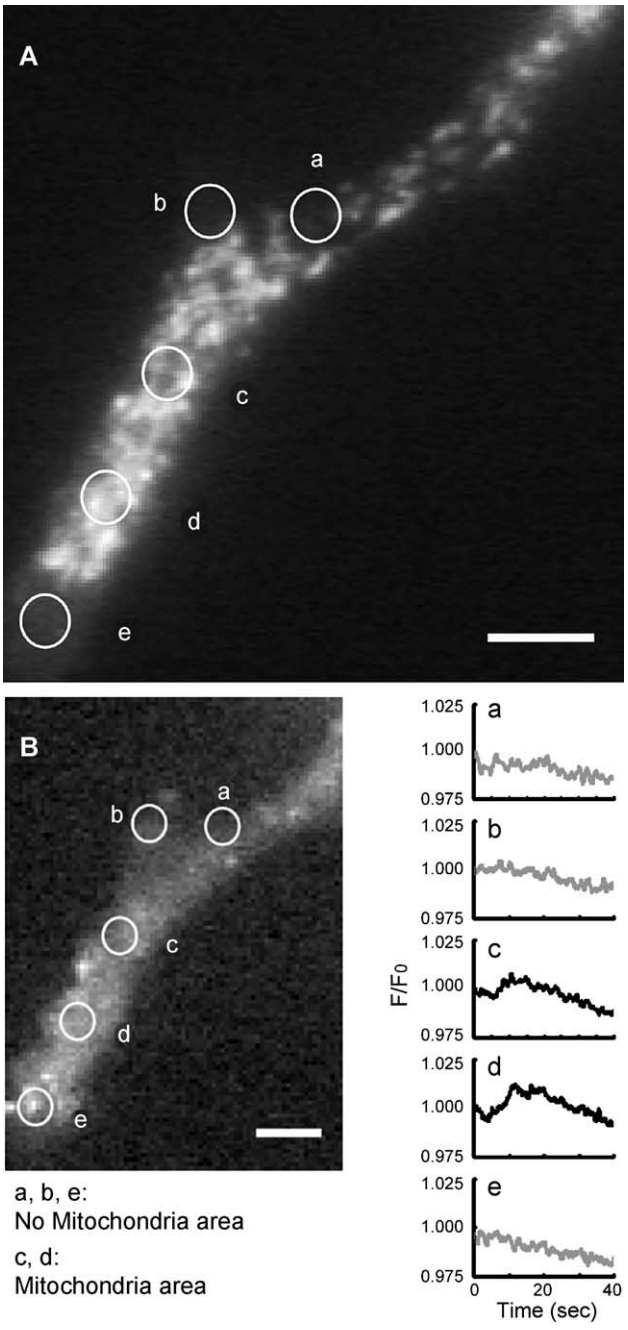

Fig. 4. Mg^{2+} release on the mitochondria. (A) Localization of mitochondria at a neurite of differentiated PC12 cell was visualized with MitoFluor™ Red 589. White circles were each ROIs. Mitochondria do not exist on the ROI a, b, and e. Mitochondria were identified on the ROI c and d. The scale bar indicates 5 μm. (B) KMG-104 image and time courses of fluorescences at each ROIs, which are the same places as image A.

3.5. Mg^{2+} release from mitochondria

Localization of mitochondria and Mg^{2+} response were visualized with MitoFluor™ Red 589 and KMG-104. Fluorescences were measured at neuritis of differentiated PC12 cells to take advantage of thickness for sparse mitochondrial localization. ROIs were selected based on a viewpoint whether mitochondria exist or not (Fig. 4A). Weak

$[Mg^{2+}]_i$ increase was obtained at mitochondria localized area by 5 μM FCCP treatment (Fig. 4B; c and d), while $[Mg^{2+}]_i$ did not change at areas of no mitochondria (Fig. 4B; a, b, and e). This relation was observed in other trials (N=4). From these results, it was revealed that the Mg^{2+} store at intracellular Mg^{2+} release by FCCP treatment was mitochondria.

3.6. Mg^{2+} is released after mitochondrial depolarization

Ψ_{Mt} was visualized with JC-1 to monitor the initial timing of mitochondrial depolarization following exposure to FCCP. Cells double-stained with fura-2 and JC-1 showed both mitochondrial depolarization and an increase in $[Ca^{2+}]_i$ (N=4, n=28) upon exposure to FCCP, with the initial take-off point of the depolarization preceding that of the Ca^{2+} increase by an average of 3.8±1.7 s (Fig. 5A, top). This difference was significant at the P<0.01 level. Similar experiments were performed with fura-2- and KMG-104-loaded cells, with the initial take-off point of $[Ca^{2+}]_i$ being slightly faster than that of $[Mg^{2+}]_i$ (Fig. 5A, bottom). Here, the lag between Ca^{2+} and Mg^{2+} was 1.9±2.4 s, with this difference also being significant at the P<0.01 level (N=4, n=33). These results show that the sequence of events was mitochondrial depolarization first, followed by an increase in $[Ca^{2+}]_i$, and then an increase in $[Mg^{2+}]_i$ (Fig. 5B). Taking into account all of the above, we conclude that the mitochondria serve as the intracellular Mg^{2+} store in PC12 cells, with depolarization of the mitochondrial membrane triggering the increase in $[Mg^{2+}]_i$.

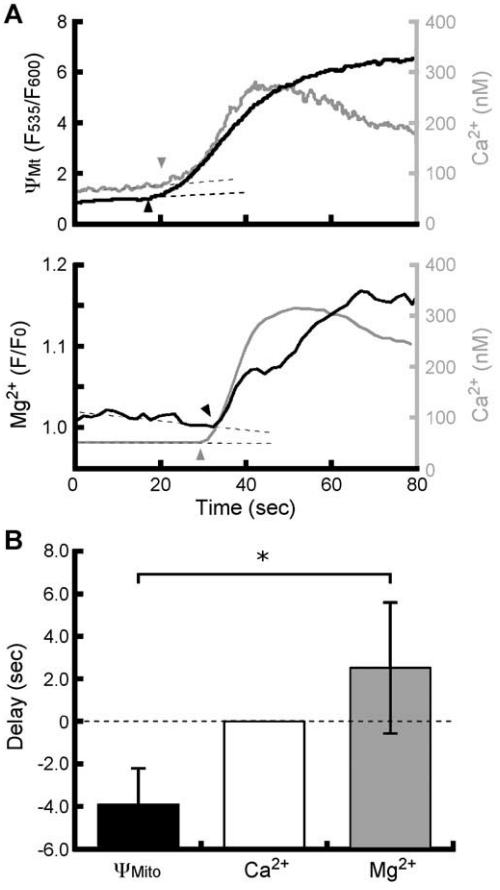

Fig. 5. Mitochondrial membrane depolarization precedes $[Mg^{2+}]_i$ Increase. (A) Time courses of mitochondrial membrane depolarization and $[Ca^{2+}]_i$ increase (top), and $[Ca^{2+}]_i$ and $[Mg^{2+}]_i$ increase (bottom). Arrowheads indicate commencement of rising. (B) Bar graph describing start point of timing for each parameter, with data normalized to the start point of timing of the increase in $[Ca^{2+}]_i$ (white bar). The onset of mitochondrial depolarization (black bar) occurred earlier than that of the increase in $[Ca^{2+}]_i$, which in turn preceded that of the increase in $[Mg^{2+}]_i$ (grey bar). Error bars show S.D., with the asterisk signifying P<0.01 (Student's t test).

4. Discussion

We have demonstrated here that mitochondria in PC12 cells play a role as intracellular Mg^{2+} stores. Isolated mitochondria were used in previous reports concerning mitochondrial Mg^{2+} accumulation and/or release [51–53]. This report also presents results showing that mitochondrial Mg^{2+} release occurs upon mitochondrial depolarization in whole cells. The simultaneous measurement of $[Ca^{2+}]_i$ is important because it confirms not only the nature of the relationship between Ca^{2+} and Mg^{2+} mobilization but also the viability of the cells being tested. While exposure to FCCP induced an increase in $[Mg^{2+}]_i$ in PC12 cells, the double staining method and direct liberation of caged Ca^{2+} or IP_3 with laser photolysis revealed that there is no form of Ca^{2+}-induced Mg^{2+} release from ER. While ER Mg^{2+} uptake [54] has been reported, Mg^{2+} release via Ca^{2+}-activated receptors was not observed in the present experiments. Oligomycin pretreatment of cells and estimation of [ATP] revealed that FCCP did not induce the release of Mg^{2+} from Mg-ATP in the initial 2 min of exposure. Because all responses in this study occurred in 2 min from stimulation, they were not ATP consumption. The source of Mg^{2+} in the FCCP-induced increase in $[Mg^{2+}]_i$ was therefore mitochondria given that the increase followed that of mitochondrial membrane depolarization. We successfully displayed in whole living cells the mitochondrial Mg^{2+} release mechanisms with fluorescent indicators.

4.1. Mitochondrial Mg^{2+} accumulation and release mechanism

Mg^{2+} accumulation in the mitochondria has been previously confirmed by EPMA, where the Mg^{2+} contents of mitochondria and cytoplasm were 101 and 116 mmol/kg dry wt, respectively, in undifferentiated HL-60 cells [36,55]. However, these values include both free and not free Mg^{2+}, and it is expected that much of the intracellular Mg^{2+} exists in the mitochondria. One mechanism for mitochondrial Mg^{2+} accumulation is that of the Mg-ATP^{2-}/Pi^{2-} carrier [56], which exchanges cytoplasmic Mg-ATP^{2-} for mitochondrial HPO_4^{2-}. Recently, Mrs2 protein, which is a component of an

Mg^{2+}-selective ion channel, was reported in yeast mitochondria, [57,58]. The driving force for Mg^{2+} accumulation via this channel is the mitochondrial inner membrane potential. This mechanism resembles that of Ca^{2+} accumulation in the mitochondria, where a Ca^{2+} uniporter uses the electrochemical gradient of inner membrane to transport Ca^{2+} against its concentration gradient [37,59]. If mammalian cells possess a similar protein, then this could provide a cue for understanding mitochondrial Mg^{2+} accumulation mechanisms.

The rate of increase of $[Ca^{2+}]_i$ observed in the present experiments was steeper than that seen for the increase in $[Mg^{2+}]_i$ (Fig. 1B and C). This difference implies that Mg^{2+} release and Ca^{2+} release operate under different mechanisms. Mitochondria possess both Na^+-dependent (Na^+/Ca^{2+} exchangers) and Na^+-independent (H^+/Ca^{2+} exchangers and Ca^{2+} uniporters) Ca^{2+} efflux mechanisms [38]. However, the manner in which Mg^{2+} leaks from the mitochondria has not yet been identified. Because the Mg^{2+} channel made by Mrs2 protein is membrane potential-dependent in its activity [57,58], accumulated Mg^{2+} might be released through the channel by depolarization. Since the increase in $[Mg^{2+}]_i$ seen here followed that of the increase in $[Ca^{2+}]_i$, the threshold potential for Mg^{2+} channel opening in the mitochondria might be higher than that of Ca^{2+} channels. The difference in the rate of $[Ca^{2+}]_i$ and $[Mg^{2+}]_i$ increase following FCCP treatment might reflect differences in the intramitochondrial and cytosolic concentrations of these ions.

Depolarization of Ψ_{Mt} is often induced by the opening of mitochondria permeability transition pore (PTP) [60]. When the PTP opens, cytochrome *c* is released from mitochondria, and this triggers one of the pre-processes of cell apoptosis [61]. Because apoptosis and $[Mg^{2+}]_i$ increase are linked at the stage of depolarization of Ψ_{Mt}, some apoptotic inducible factors might increase $[Mg^{2+}]_i$.

4.2. Mg^{2+} in relation to mitochondrial function and disease states

Mg^{2+} and mitochondria have been implicated in a number of disease states. Parkinson's disease (PD), for example, is one of the most common neurodegenerative disorders and one in which $[Mg^{2+}]_i$ was reported to be lower in the cortex than in the white matter of PD brains [62], and where alterations to mitochondrial function have been implicated [63,64]. If mitochondrial $[Mg^{2+}]_i$ regulation is affected by mitochondrial dysfunction, then a low $[Mg^{2+}]_i$ in cells could result. This could be one reason for low Mg^{2+}-related diseases such as hypertension or diabetes mellitus. Given that we have elucidated aspects of the relation between Mg^{2+} and mitochondria in this study, these findings could give rise to a deeper understanding of the mechanisms underlying some disease states.

In conclusion, we have demonstrated here the presence of mitochondrial Mg^{2+} release in response to depolarization of the mitochondrial membrane. As these results show that the mitochondria serve as intracellular Mg^{2+} stores, a deeper understanding of the mechanisms of Mg^{2+} mobilization and $[Mg^{2+}]$ in disease states could result.

Acknowledgements

This research was supported in part by the Ministry of Education, Culture, Sports, Science and Technology, Grant-in-Aid for the 21st Century Center of Excellence (COE) Program entitled "Understanding and Control of Life's Function via Systems Biology (Keio University)", and by Special Coordination Funds for Promoting Science and Technology.

References

[1] J.A. Subirana, M. Soler-Lopez, Cations as hydrogen bond donors: a view of electrostatic interactions in DNA, Annu. Rev. Biophys. Biomol. Struct. 32 (2003) 27–45.
[2] P. Brion, E. Westhof, Hierarchy and dynamics of RNA folding, Annu. Rev. Biophys. Biomol. Struct. 26 (1997) 113–137.
[3] C.A. Vandenberg, Inward rectification of a potassium channel in cardiac ventricular cells depends on internal magnesium ions, Proc. Natl. Acad. Sci. U. S. A. 84 (1987) 2560–2564.
[4] H. Matsuda, A. Saigusa, H. Irisawa, Ohmic conductance through the inwardly rectifying K channel and blocking by internal Mg^{2+}, Nature 325 (1987) 156–159.
[5] M.L. Mayer, G.L. Westbrook, P.B. Guthrie, Voltage-dependent block by Mg^{2+} of NMDA responses in spinal cord neurones, Nature 309 (1984) 261–263.
[6] L. Nowak, P. Bregestovski, P. Ascher, A. Herbet, A. Prochiantz, Magnesium gates glutamate-activated channels in mouse central neurones, Nature 307 (1984) 462–465.
[7] A.M. Romani, A. Scarpa, Regulation of cellular magnesium, Front. Biosci. 5 (2000) D720–D734.
[8] A. Romani, A. Scarpa, Regulation of cell magnesium, Arch. Biochem. Biophys. 298 (1992) 1–12.
[9] J. Zhao, W.N. Wang, Y.C. Tan, Y. Zheng, Z.X. Wang, Effect of Mg^{2+} on the kinetics of guanine nucleotide binding and hydrolysis by Cdc42, Biochem. Biophys. Res. Commun. 297 (2002) 653–658.
[10] A. Hirata, F. Hirata, DNA chain unwinding and annealing reactions of lipocortin (annexin) I heterotetramer: regulation by Ca^{2+} and Mg^{2+}, Biochem. Biophys. Res. Commun. 291 (2002) 205–209.
[11] Y.H. Ko, S. Hong, P.L. Pedersen, Chemical mechanism of ATP synthase. Magnesium plays a pivotal role in formation of the transition state where ATP is synthesized from ADP and inorganic phosphate, J. Biol. Chem. 274 (1999) 28853–28856.
[12] N.E. Saris, E. Mervaala, H. Karppanen, J.A. Khawaja, A. Lewenstam, Magnesium. An update on physiological, clinical and analytical aspects, Clin. Chim. Acta 294 (2000) 1–26.
[13] R. Lopez-Ridaura, W.C. Willett, E.B. Rimm, S. Liu, M.J. Stampfer, J.E. Manson, F.B. Hu, Magnesium intake and risk of type 2 diabetes in men and women, Diabetes Care 27 (2004) 134–140.

[14] R. Vink, C.A. O'Connor, A.J. Nimmo, D.L. Heath, Magnesium attenuates persistent functional deficits following diffuse traumatic brain injury in rats, Neurosci. Lett. 336 (2003) 41–44.
[15] R.M. Touyz, E.L. Schiffrin, Activation of the Na^+–H^+ exchanger modulates angiotensin II-stimulated Na^+-dependent Mg^{2+} transport in vascular smooth muscle cells in genetic hypertension, Hypertension 34 (1999) 442–449.
[16] L.M. Resnick, R.K. Gupta, J.H. Laragh, Intracellular free magnesium in erythrocytes of essential hypertension: relation to blood pressure and serum divalent cations, Proc. Natl. Acad. Sci. U. S. A. 81 (1984) 6511–6515.
[17] G. Paolisso, M. Barbagallo, Hypertension, diabetes mellitus, and insulin resistance: the role of intracellular magnesium, Am. J. Hypertens. 10 (1997) 346–355.
[18] T. Gunther, J. Vormann, Mg^{2+} efflux is accomplished by an amiloride-sensitive Na^+/Mg^{2+} antiport, Biochem. Biophys. Res. Commun. 130 (1985) 540–545.
[19] T. Gunther, J. Vormann, Characterization of Na^+/Mg^{2+} antiport by simultaneous $^{28}Mg^{2+}$ influx, Biochem. Biophys. Res. Commun. 148 (1987) 1069–1074.
[20] P.W. Flatman, Mechanisms of magnesium transport, Annu. Rev. Physiol. 53 (1991) 259–271.
[21] P.W. Flatman, L.M. Smith, Sodium-dependent magnesium uptake by ferret red cells, J. Physiol. 443 (1991) 217–230.
[22] C. Cefaratti, A. Romani, A. Scarpa, Characterization of two Mg^{2+} transporters in sealed plasma membrane vesicles from rat liver, Am. J. Physiol. 275 (1998) C995–C1008.
[23] C. Cefaratti, A. Romani, A. Scarpa, Differential localization and operation of distinct Mg^{2+} transporters in apical and basolateral sides of rat liver plasma membrane, J. Biol. Chem. 275 (2000) 3772–3780.
[24] T. Kubota, K. Tokuno, J. Nakagawa, Y. Kitamura, H. Ogawa, Y. Suzuki, K. Suzuki, K. Oka, Na^+/Mg^{2+} transporter acts as a Mg^{2+} buffering mechanism in PC12 cells, Biochem. Biophys. Res. Commun. 303 (2003) 332–336.
[25] A. Leyssens, A.V. Nowicky, L. Patterson, M. Crompton, M.R. Duchen, The relationship between mitochondrial state, ATP hydrolysis, $[Mg^{2+}]_i$ and $[Ca^{2+}]_i$ studied in isolated rat cardiomyocytes, J. Physiol. 496 (1996) 111–128.
[26] G.H. Zhang, J.E. Melvin, Secretagogue-induced mobilization of an intracellular Mg^{2+} pool in rat sublingual mucous acini, J. Biol. Chem. 267 (1992) 20721–20727.
[27] F. Munoz, M.E. Martin, M. Salinas, J.L. Fando, Carbonyl cyanide *p*-trifluoromethoxyphenylhydrazone (FCCP) induces initiation factor 2 alpha phosphorylation and translation inhibition in PC12 cells, FEBS Lett. 492 (2001) 156–159.
[28] L.L. Haak, M. Grimaldi, S.S. Smaili, J.T. Russell, Mitochondria regulate Ca^{2+} wave initiation and inositol trisphosphate signal transduction in oligodendrocyte progenitors, J. Neurochem. 80 (2002) 405–415.
[29] S. Koizumi, M.D. Bootman, L.K. Bobanovic, M.J. Schell, M.J. Berridge, P. Lipp, Characterization of elementary Ca^{2+} release signals in NGF-differentiated PC12 cells and hippocampal neurons, Neuron 22 (1999) 125–137.
[30] J. Mironneau, F. Coussin, L.H. Jeyakumar, S. Fleischer, C. Mironneau, N. Macrez, Contribution of ryanodine receptor subtype 3 to Ca^{2+} responses in Ca^{2+}-overloaded cultured rat portal vein myocytes, J. Biol. Chem. 276 (2001) 11257–11264.
[31] K.E. Fogarty, J.F. Kidd, D.A. Tuft, P. Thorn, Mechanisms underlying $InsP_3$-evoked global Ca^{2+} signals in mouse pancreatic acinar cells, J. Physiol. 526 (2000) 515–526.
[32] J.D. Johnson, R.J. Nakkula, C. Vasulka, L.B. Smillie, Modulation of Ca^{2+} exchange with the Ca^{2+}-specific regulatory sites of troponin C, J. Biol. Chem. 269 (1994) 8919–8923.
[33] J.P. Davis, J.A. Rall, P.J. Reiser, L.B. Smillie, S.B. Tikunova, Engineering competitive magnesium binding into the first EF-hand of skeletal troponin C, J. Biol. Chem. 277 (2002) 49716–49726.
[34] I. Kameshita, H. Fujisawa, Detection of calcium binding proteins by two-dimensional sodium dodecyl sulfate-polyacrylamide gel electrophoresis, Anal. Biochem. 249 (1997) 252–255.
[35] R.G. Eckenhoff, A.P. Somlyo, Cardiac mitochondrial calcium content during fatal doxorubicin toxicity, Toxicol. Appl. Pharmacol. 97 (1989) 167–172.
[36] A. Di Francesco, R.W. Desnoyer, V. Covacci, F.I. Wolf, A. Romani, A. Cittadini, M. Bond, Changes in magnesium content and subcellular distribution during retinoic acid-induced differentiation of HL60 cells, Arch. Biochem. Biophys. 360 (1998) 149–157.
[37] T.E. Gunter, L. Buntinas, G. Sparagna, R. Eliseev, K. Gunter, Mitochondrial calcium transport: mechanisms and functions, Cell Calcium 28 (2000) 285–296.
[38] V.Y. Ganitkevich, The role of mitochondria in cytoplasmic Ca^{2+} cycling, Exp. Physiol. 88 (2003) 91–97.
[39] Y. Kirichok, G. Krapivinsky, D.E. Clapham, The mitochondrial calcium uniporter is a highly selective ion channel, Nature 427 (2004) 360–364.
[40] H. Komatsu, N. Iwasawa, D. Citterio, Y. Suzuki, T. Kubota, K. Tokuno, Y. Kitamura, K. Oka, K. Suzuki, Design and synthesis of highly-sensitive and -selective fluorescein-derived magnesium fluorescent probes and application to intracellular 3D-Mg^{2+} imaging, J. Am. Chem. Soc. (in press).
[41] H. Komatsu, T. Kubota, K. Oka, K. Suzuki, Simultaneous fluorescent imaging of intracellular calcium and magnesium ions, Pittcon 2004 (2004) 12200–200.
[42] L.A. Greene, A.S. Tischler, Establishment of a noradrenergic clonal line of rat adrenal pheochromocytoma cells which respond to nerve growth factor, Proc. Natl. Acad. Sci. U. S. A. 73 (1976) 2424–2428.
[43] Y. Suzuki, H. Komatsu, T. Ikeda, N. Saito, S. Araki, D. Citterio, D. Hisamoto, Y. Kitamura, T. Kubota, J. Nakagawa, K. Oka, K. Suzuki, Design and synthesis of Mg^{2+}-selective fluoroionophores based on a coumarin derivative and application for Mg^{2+} measurement in a living cell, Anal. Chem. 74 (2002) 1423–1428.
[44] M. Zhao, S. Hollingworth, S.M. Baylor, Properties of tri- and tetracarboxylate Ca^{2+} indicators in frog skeletal muscle fibers, Biophys. J. 70 (1996) 896–916.
[45] G. Grynkiewicz, M. Poenie, R.Y. Tsien, A new generation of Ca^{2+} indicators with greatly improved fluorescence properties, J. Biol. Chem. 260 (1985) 3440–3450.
[46] S.T. Smiley, M. Reers, C. Mottola-Hartshorn, M. Lin, A. Chen, T.W. Smith, G.D. Steele Jr., L.B. Chen, Intracellular heterogeneity in mitochondrial membrane potentials revealed by a J-aggregate-forming lipophilic cation JC-1, Proc. Natl. Acad. Sci. U. S. A. 88 (1991) 3671–3675.
[47] M.N. Sharikabad, K.M. Ostbye, O. Brors, Increased $[Mg^{2+}]_o$ reduces Ca^{2+} influx and disruption of mitochondrial membrane potential during reoxygenation, Am. J. Physiol., Heart Circ. Physiol. 281 (2001) H2113–H2123.
[48] P.E. Stanley, S.G. Williams, Use of the liquid scintillation spectrometer for determining adenosine triphosphate by the luciferase enzyme, Anal. Biochem. 29 (1969) 381–392.
[49] S. Kudo, R. Morigaki, J. Saito, M. Ikeda, K. Oka, K. Tanishita, Shear-stress effect on mitochondrial membrane potential and albumin uptake in cultured endothelial cells, Biochem. Biophys. Res. Commun. 270 (2000) 616–621.
[50] M.M. Bradford, A rapid and sensitive method for the quantitation of microgram quantities of protein utilizing the principle of protein-dye binding, Anal. Biochem. 72 (1976) 248–254.
[51] G.P. Brierley, M. Davis, D.W. Jung, Respiration-dependent uptake and extrusion of Mg^{2+} by isolated heart mitochondria, Arch. Biochem. Biophys. 253 (1987) 322–332.
[52] G.A. Rutter, N.J. Osbaldeston, J.G. McCormack, R.M. Denton, Measurement of matrix free Mg^{2+} concentration in rat heart

mitochondria by using entrapped fluorescent probes, Biochem. J. 271 (1990) 627–634.
[53] M. Salvi, A. Bozac, A. Toninello, Gliotoxin induces Mg^{2+} efflux from intact brain mitochondria, Neurochem. Int. 45 (2004) 759–764.
[54] O. Baumann, B. Walz, A.V. Somlyo, A.P. Somlyo, Electron probe microanalysis of calcium release and magnesium uptake by endoplasmic reticulum in bee photoreceptors, Proc. Natl. Acad. Sci. U. S. A. 88 (1991) 741–744.
[55] M. Bond, G. Vadasz, A.V. Somlyo, A.P. Somlyo, Subcellular calcium and magnesium mobilization in rat liver stimulated in vivo with vasopressin and glucagon, J. Biol. Chem. 262 (1987) 15630–15636.
[56] J.R. Aprille, Mechanism and regulation of the mitochondrial ATP-Mg/P_i carrier, J. Bioenerg. Biomembranes 25 (1993) 473–481.
[57] G. Zsurka, J. Gregan, R.J. Schweyen, The human mitochondrial Mrs2 protein functionally substitutes for its yeast homologue, a candidate magnesium transporter, Genomics 72 (2001) 158–168.
[58] M. Kolisek, G. Zsurka, J. Samaj, J. Weghuber, R.J. Schweyen, M. Schweigel, Mrs2p is an essential component of the major electrophoretic Mg^{2+} influx system in mitochondria, EMBO J. 22 (2003) 1235–1244.
[59] K. Medler, E.L. Gleason, Mitochondrial Ca^{2+} buffering regulates synaptic transmission between retinal amacrine cells, J. Neurophysiol. 87 (2002) 1426–1439.
[60] P. Bernardi, Modulation of the mitochondrial cyclosporin A-sensitive permeability transition pore by the proton electrochemical gradient. Evidence that the pore can be opened by membrane depolarization, J. Biol. Chem. 267 (1992) 8834–8839.
[61] M. Di Paola, T. Cocco, M. Lorusso, Arachidonic acid causes cytochrome *c* release from heart mitochondria, Biochem. Biophys. Res. Commun. 277 (2000) 128–133.
[62] M. Yasui, T. Kihira, K. Ota, Calcium, magnesium and aluminum concentrations in Parkinson's disease, Neurotoxicology 13 (1992) 593–600.
[63] T.B. Sherer, R. Betarbet, A.K. Stout, S. Lund, M. Baptista, A.V. Panov, M.R. Cookson, J.T. Greenamyre, An in vitro model of Parkinson's disease: linking mitochondrial impairment to altered alpha-synuclein metabolism and oxidative damage, J. Neurosci. 22 (2002) 7006–7015.
[64] M. Orth, A.H. Schapira, Mitochondrial involvement in Parkinson's disease, Neurochem. Int. 40 (2002) 533–541.